

# Transport across the blood-brain-barrier may be limiting for hyperpolarized [1-<sup>13</sup>C]pyruvate neuro-oncology studies

Jack Julian James Jenkins Miller<sup>1,2,3</sup>, James Larkin<sup>4</sup>, Katherine R Fisher<sup>1</sup>, Vicky Ball<sup>1</sup>, Kevin J Ray<sup>4</sup>, Sebastien Serres<sup>5</sup>, Damian John Tyler<sup>1,2</sup>, Angus Zoen Lau<sup>1,6</sup>, and Nicola Ruth Sibson<sup>4</sup>

<sup>1</sup>Department of Physiology, Anatomy & Genetics, University of Oxford, Oxford, United Kingdom, <sup>2</sup>Oxford Centre for Clinical Magnetic Resonance Research, University of Oxford, Oxford, United Kingdom, <sup>3</sup>Department of Physics, University of Oxford, Oxford, United Kingdom, <sup>4</sup>Cancer Research UK and Medical Research Council Oxford Institute for Radiation Oncology, University of Oxford, Oxford, United Kingdom, <sup>5</sup>School of Life Sciences, University of Nottingham, Nottingham, United Kingdom, <sup>6</sup>Physical Sciences, Sunnybrook Research Institute, Toronto, ON, Canada

## Synopsis

**Hyperpolarized pyruvate has previously been used to probe primary brain cancer. Through imaging the delivery and metabolism of both hyperpolarized [1-<sup>13</sup>C]pyruvate and ethyl-[1-<sup>13</sup>C]pyruvate in a rodent model of cancer metastasis to the brain, we show that the transport of [1-<sup>13</sup>C]pyruvate across the blood brain barrier may be limiting until it is compromised by metastatic cell infiltration.**

## Purpose

Both hyperpolarized [1-<sup>13</sup>C]pyruvate and lipophilic ethyl-[1-<sup>13</sup>C]pyruvate have been used to monitor tumour metabolism in the brain.<sup>[1,2]</sup> However, studies to date have probed primary brain cancers (e.g. glioblastoma<sup>[3]</sup>) and not brain metastases, which, with a survival time of 2-4 months, pose a significant unmet clinical need.<sup>[4]</sup> We therefore investigated the feasibility of detecting induced cancer metastases to the brain using dissolution-Dynamic Nuclear Polarization (DNP) with either [1-<sup>13</sup>C]pyruvate or ethyl-[1-<sup>13</sup>C]pyruvate. As the disruption of the blood-brain-barrier (BBB) occurs by angiogenesis four weeks after induction, we additionally compared pyruvate active transport to the Fick-driven diffusion of ethyl-[1-<sup>13</sup>C]pyruvate across the intact and disrupted BBB.

## Methods

**Animal model:** Female BD-IX rats ( $n = 4$ ) were anaesthetised (isoflurane) and stereotactically injected intra-cerebrally with ENU-1564 cells to provide a well-characterised model of secondary brain metastases;<sup>[5]</sup> controls were injected with saline. Rats were scanned weekly post-surgery with both hyperpolarized probes and post-gadolinium proton gradient echo T<sub>1</sub>-weighted images (80 × 80 mm FOV; 192 × 192 matrix; 1.5 mm thick; 120 ms TR; 3.8 ms TE; 7T Varian system) were acquired to assess tumour burden. Animals were provided with analgesia and monitored daily; all experiments were performed following ethical approval.

**[1-<sup>13</sup>C]Pyruvate imaging:** A flyback 3D spectral-spatial EPI sequence (37.5 mm slab excite; 64 × 64 mm<sup>2</sup> FOV; volume <sup>13</sup>C transmit/surface receive; TR 150 ms; TE 12.18 ms) was designed and reconstructed as described previously<sup>[6]</sup> at 2 × 2 × 4 mm<sup>3</sup>. 31 mg of [1-<sup>13</sup>C]pyruvate with OX063 radical was polarized in a prototype hyperpolarizer for 45 minutes prior to dissolution as described previously,<sup>[7]</sup> and injection of 2 ml 80 mmol pyruvate over 20 s via a tail vein cannula. Hyperpolarized pyruvate/bicarbonate/lactate volumes were acquired interleaved (TR = 1.8 s/volume; total FA = 17°, 61°, 61°).

**Ethyl-[1-<sup>13</sup>C]Pyruvate imaging:** A spiral multiecho sequence was designed with echo times to maximise the total effective number of signal averages (30 mm sinc excitation; 80 × 80 mm<sup>2</sup> FOV; 0.5 s TR; 8 echoes; TE = 1.05, 1.59, 2.13, 2.67, 3.21, 3.75, 4.29, 4.83, with FID 64 ms, FA/shot = 15°). Ethyl-[1-<sup>13</sup>C]pyruvate (Isotec) was doped with 5 μL/10 mM Gd-DPTA in ethanol and 15 mM AH111501 radical (GE Healthcare), which was found to be more soluble than OX063. Ethyl-[1-<sup>13</sup>C] pyruvate was then hyperpolarized in a prototype hyperpolarizer at 94 GHz for approximately 2.5 hours prior to dissolution. 2 mL was injected over 20 s via tail vein cannula. Data were reconstructed by a pre-measured gradient impulse response function<sup>[7]</sup> followed by NUFFT<sup>[8]</sup> for a reconstructed resolution of 3.125 × 3.125 mm<sup>2</sup> (PSF FWHM).

## Results

Hyperpolarized [1-<sup>13</sup>C]pyruvate was visible predominantly in the cerebral circulation (Fig. 1). Lactate following pyruvate injection predominantly colocalized to and near major vessels in healthy animals, and in tumour once the BBB was disrupted.

The use of AH111501 meant that ethyl-[1-<sup>13</sup>C]pyruvate polarized to a higher degree than reported previously,<sup>[2]</sup> with limiting solid-state polarization ~ 70% that of pyruvate. Uniform perfusion of ethyl-[1-<sup>13</sup>C]-pyruvate was observed in the brain, in contrast to pyruvate (Fig. 2), indicating greater transport. Downstream production of [1-<sup>13</sup>C]pyruvate from hyperpolarized ethyl-[1-<sup>13</sup>C]-pyruvate was also visible approximately homogeneously within the brain. Lactate production from ethyl-[1-<sup>13</sup>C]-pyruvate was only visible in the region of the tumour, and not elsewhere, in contrast to the vascular production following infusion of [1-<sup>13</sup>C]-pyruvate. It was not possible to detect hyperpolarized lactate following infusion of either probe until tumours had become angiogenic (at 4 weeks), and therefore also visible to gadolinium.

## Discussion

We present the first high-resolution investigation of secondary brain cancer with hyperpolarized probes. Previous work using [1-<sup>13</sup>C]pyruvate has imaged primary brain cancer at comparatively modest spatial resolution, e.g. 5 × 5 × 10 mm<sup>3</sup>.<sup>[9]</sup> We only observed lactate production following injection of [1-<sup>13</sup>C]pyruvate in voxels containing a blood vessel, which indicates that partial volume effects cannot be neglected in such studies. The SNR from ethyl-[1-<sup>13</sup>C]pyruvate originated intracellular pyruvate in the brain is substantially higher than that of hyperpolarized [1-<sup>13</sup>C]pyruvate. The distinct spatial localization of [1-<sup>13</sup>C]pyruvate within the brain following intravenous injection of ethyl-[1-<sup>13</sup>C]pyruvate suggests that the rate of transport of hyperpolarized [1-<sup>13</sup>C]pyruvate across the BBB is limiting, and that ethyl-[1-<sup>13</sup>C]pyruvate is potentially a more sensitive hyperpolarized probe. This is consistent with radioisotope measurements of <sup>14</sup>C-pyruvate transport in the rat brain being

approximately 100-fold slower than in the rodent heart (Michaelis-Menten  $V_{\max} = 0.18 \mu\text{mol min}^{-1} \text{g}^{-1}$  in the brain vs  $V_{\max} \approx 10 \mu\text{mol min}^{-1} \text{g}^{-1}$  in the heart).<sup>[10,11]</sup> Whilst neither hyperpolarized  $[1-^{13}\text{C}]$ pyruvate nor ethyl- $[1-^{13}\text{C}]$ pyruvate could resolve brain metastases until angiogenesis, the higher apparent transport rate of ethyl- $[1-^{13}\text{C}]$ pyruvate and lack of background indicates its use for future studies, such as guiding radiotherapy to metabolically active areas of tumour.

## Conclusions and Further Work

Hyperpolarized ethyl- $[1-^{13}\text{C}]$ pyruvate may be a more attractive metabolic probe for neuro-oncology applications, owing to its ability to cross the intact BBB and produce intracellular pyruvate. Small animal studies of  $[1-^{13}\text{C}]$ pyruvate may have been confounded by partial volume effects, as transport within the lifetime of the hyperpolarized experiment is low. Further work will quantify these effects with BBB permeabilizing agents, and also use (ethyl- $[1-^{13}\text{C}]$ pyruvate to monitor disease.

## Acknowledgements

The authors would like thank financial support from Cancer Research UK (Grant number: C5255/A12678), St. Hugh's College, Oxford, and an EPSRC Doctoral Training Centre Grant and Doctoral Prize Fellowship (refs. EP/J013250/1 and EP/M508111/1). We also acknowledge financial support from the British Heart Foundation (Fellowships FS/10/002/28078 & FS/11/50/29038, Programme Grant RG/11/9/28921) and NVidia corporation for the gift of a GPU.

## References

- [1] I. Park, R. Bok, T. Ozawa, J. J. Phillips, C. D. James, D. B. Vigneron, S. M. Ronen, S. J. Nelson, J. Magn. Reson. Imaging June 2011, 33, 1284–90.
- [2] R. E. Hurd, Y.-F. Yen, D. Mayer, A. Chen, D. Wilson, S. Kohler, R. Bok, D. Vigneron, J. Kurhanewicz, J. Tropp, D. Spielman, A. Pfefferbaum, Magn. Reson. Med. May 2010, 63, 1137–43. 2
- [3] I. Park, S. Hu, R. Bok, T. Ozawa, M. Ito, J. Mukherjee, J. J. Phillips, C. D. James, R. O. Pieper, S. M. Ronen, D. B. Vigneron, S. J. Nelson, Magn. Reson. Med. July 2013, 70, 33–39.
- [4] A. F. Eichler, E. Chung, D. P. Kodack, J. S. Loeffler, D. Fukumura, R. K. Jain, Nat. Rev. Clin. Oncol. June 2011, 8, 344–356.
- [5] S. Serres, C. J. Martin, M. Sarmiento Soto, C. Bristow, E. R. O'Brien, J. J. Connell, A. A. Khrapitchev, N. R. Sibson, Int. J. Cancer Feb. 2014, 134, 885–96.
- [6] J. J. Miller, A. Z. Lau, I. Teh, J. E. Schneider, P. Kinchesh, S. Smart, V. Ball, N. R. Sibson, D. J. Tyler, Magn. Reson. Med. May 2015, 75, 1515–1524.
- [7] J. H. Duyn, Y. Yang, J. A. Frank, J. W. van der Veen, J. Magn. Reson. May 1998, 132, 150–3.
- [8] J. Fessler, B. Sutton, IEEE Trans. Signal Process. Feb. 2003, 51, 560–574.
- [9] I. Park, P. E. Z. Larson, M. L. Zierhut, S. Hu, R. Bok, T. Ozawa, J. Kurhanewicz, D. B. Vigneron, S. R. Vandenberg, C. D. James, S. J. Nelson, en, Neuro. Oncol. Feb. 2010, 12, 133–44.
- [10] J. E. Cremer, V. J. Cunningham, W. M. Pardridge, L. D. Braun, W. H. Oldendorf, J. Neurochem. Aug. 1979, 33, 439–45.
- [11] S. C. Dennis, M. C. Kohn, M. B. Slegowski, G. J. Anderson, D. Garfinkel, Adv. Myocardiol. Jan. 1985, 6, 259–72.

## Figures

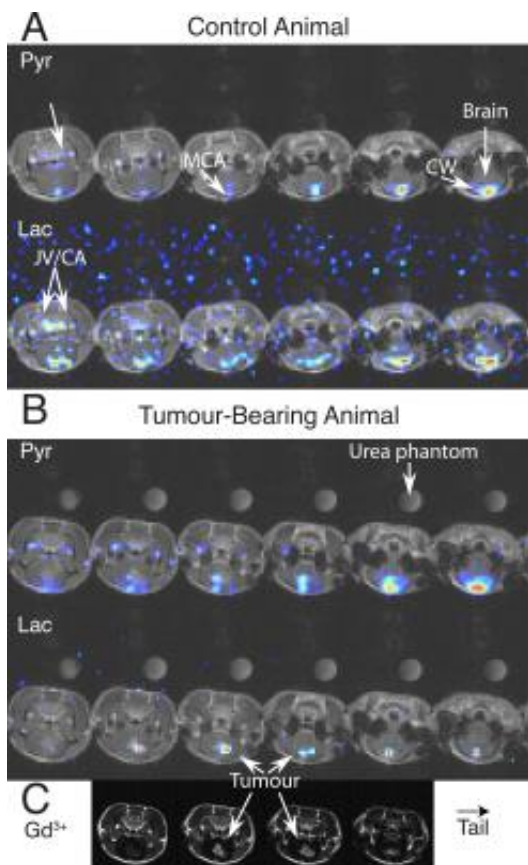


Fig. 1: Hyperpolarized [ $1\text{-}^{13}\text{C}$ ]pyruvate production visible at high resolution in the rat brain, in both a representative control (**A**) and affected (**B**) animals. Pyruvate was observed perfusing the Jugular vein/carotid arteries (JV/CA), middle cerebral artery (MCA) and in the Circle of Willis (CW). Lactate was predominantly observed in these regions, or in tumours, as determined by Gadolinium-DPTA contrast (**C**).

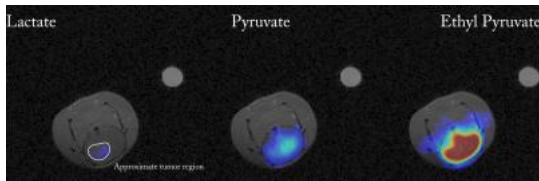


Fig. 2: Single-slice visible hyperpolarized lactate and pyruvate production after injection of ethyl pyruvate. Pyruvate production is visible in the brain only, with lactate in the rim of the metastatic tumour. A  $^{13}\text{C}$ -urea frequency reference is visible; data are summed over time.